Retinal bioavailability and functional effects of a synthetic very-long-chain polyunsaturated fatty acid in mice

Aruna Gorusupudi[a], Rameshu Rallabandi[b], Binxing Li[a], Ranganathan Arunkumar[a], J. David Blount[a], Gregory T. Rognon[a], Fu-Yen Chang[a], Alexander Wade[b], Steven Lucas[b], John C. Conboy[b], Jon D. Rainier[b], and Paul S. Bernstein[a,1]

[a]Department of Ophthalmology and Visual Sciences, John A. Moran Eye Center, Salt Lake City, UT 84132; and [b]Department of Chemistry, University of Utah, Salt Lake City, UT 84112

Edited by Janet R. Sparrow, Columbia University Medical Center, New York, NY, and accepted by Editorial Board Member Jeremy Nathans January 6, 2021 (received for review August 26, 2020)

Rare, nondietary very-long-chain polyunsaturated fatty acids (VLC-PUFAs) are uniquely found in the retina and a few other vertebrate tissues. These special fatty acids play a clinically significant role in retinal degeneration and development, but their physiological and interventional research has been hampered because pure VLC-PUFAs are scarce. We hypothesize that if Stargardt-3 or age-related macular degeneration patients were to consume an adequate amount of VLC-PUFAs that could be directly used in the retina, it may be possible to bypass the steps of lipid elongation mediated by the retina's ELOVL4 enzyme and to delay or prevent degeneration. We report the synthesis of a VLC-PUFA (32:6 n-3) in sufficient quantity to study its bioavailability and functional benefits in the mouse retina. We acutely and chronically gavage fed wild-type mice and *Elovl4* rod–cone conditional knockout mice this synthetic VLC-PUFA to understand its bioavailability and its role in visual function. VLC-PUFA-fed wild-type and *Elovl4* conditional knockout mice show a significant increase in retinal VLC-PUFA levels in comparison to controls. The VLC-PUFA-fed mice also had improvement in the animals' visual acuity and electroretinography measurements. Further studies with synthetic VLC-PUFAs will continue to expand our understanding of the physiological roles of these unique retinal lipids, particularly with respect to their potential utility for the treatment and prevention of retinal degenerative diseases.

retina | lipid | VLC-PUFA | ELOVL4 | bioavailability

Very-long-chain polyunsaturated fatty acids (VLC-PUFAs) are a special class of lipids (C ≥ 24) that cannot be synthesized de novo in vertebrates and that are rarely consumed in normal diets. They have a unique hybrid structure with a proximal end more characteristic of typical saturated fatty acids and a distal end more characteristic of common PUFAs like docosahexaenoic acid (DHA). It is believed that these properties enhance membrane fluidity and help maintain the highly curved membrane disks of the photoreceptor outer segments, which make VLC-PUFAs of particular interest and importance (1–3). VLC-PUFAs are synthesized in vivo in the retina from specific precursors, such as eicosapentaenoic acid (EPA) and arachidonic acid, through the elongation action of an enzyme known as ELOVL4 (4). Genetic defects in *ELOVL4* result in autosomal dominant Stargardt-3 disease (STGD3) (5, 6), an early-onset inherited macular dystrophy which shares some features with the more common disorder, dry age-related macular degeneration (AMD), including foveal atrophy and increased lipofuscin in the retinal pigment epithelium (RPE). Autosomal recessive mutations in *ELOVL4* have severe phenotypes that typically result in death early in life due to disruption of skin barrier function and neurological problems secondary to low levels of saturated very-long-chain fatty acids (7–9).

Although genetic variants in *ELOVL4* are not associated with AMD risk, we have shown that AMD (10) and diabetic donor eyes (11) have low VLC-PUFAs and abnormal n-3/n-6 ratios in the macula and peripheral retina presumed to be secondary to ELOVL4 dysfunction (12) and/or deficiency of dietary precursors. Age-related ELOVL2 dysfunction that would also affect VLC-PUFA levels has been implicated in AMD risk as well (13). Our study of dietary biomarkers of lipid consumption has shown that members of a Utah family with STGD3 who consume large amounts of fish, a dietary source rich in EPA and DHA, have a milder phenotype than those who rarely consume fish (14). This result is comparable to multiple epidemiological studies, which have reported a decreased risk of advanced AMD in individuals who consume large amounts of fish in their diets (15–17). Prospective clinical trials of purified fish oil supplementation in AMD and STGD3 have been not successful, however, possibly due to inadequate enrichment with the right VLC-PUFA precursors or poor subject compliance with dietary interventions (18, 19).

We hypothesize that if STGD3 or AMD patients were to consume an adequate amount of VLC-PUFAs that could be directly used in the retina, it may be possible to bypass the steps

Significance

Very-long-chain polyunsaturated fatty acids (VLC-PUFAs) longer than 26 carbons are not present in normal vertebrate diets, yet they are uniquely found in the retina and a few other tissues, implying physiological importance of their biosynthesis from shorter-chain dietary precursors via the action of the ELOVL4 enzyme. While progress has been made by studying retinal samples from human donors and by investigating mouse models of Elovl4 dysfunction, further physiology and interventional research has been hampered by the scarcity of pure VLC-PUFAs. Here, we report the synthesis of a VLC-PUFA (32:6 n-3) in sufficient quantity to study its bioavailability in mice and to investigate its potential roles in normal retinal function and for treatment of disorders associated with VLC-PUFA deficiencies.

Author contributions: A.G., J.C.C., J.D.R., and P.S.B. designed research; A.G., R.R., B.L., R.A., J.D.B., G.T.R., F.-Y.C., A.W., and S.L. performed research; R.R., A.W., S.L., and J.D.R. contributed new reagents/analytic tools; A.G., J.D.B., and P.S.B. analyzed data; and A.G., J.D.R., and P.S.B. wrote the paper.

Competing interest statement: A.G., R.R., J.D.R., P.S.B., and the University of Utah have filed a provisional patent application on the chemical synthesis of VLC-PUFAs and their therapeutic effects.

This article is a PNAS Direct Submission. J.R.S. is a guest editor invited by the Editorial Board.

[1]To whom correspondence may be addressed. Email: paul.bernstein@hsc.utah.edu.

This article contains supporting information online at https://www.pnas.org/lookup/suppl/doi:10.1073/pnas.2017739118/-/DCSupplemental.

Published February 1, 2021.

of elongation mediated by ELOVL4 (20) and ELOVL2 (13) and delay or prevent degeneration; however, scarcity of chemically pure VLC-PUFAs has precluded further laboratory animal and clinical studies. To begin to test this hypothesis, we developed a chemical synthesis of a VLC-PUFA (32:6 n-3) in sufficient quantities to determine whether VLC-PUFAs can be delivered to the retina after oral administration in mice.

Results

VLC-PUFAs are commercially available only in very small quantities, and a published synthesis had problematic coupling and reduction reactions which use toxic metal reagents (21). Moreover, we were able to achieve only minimal yields of relatively impure materials using these protocols. We developed a high-yielding approach that uses readily available reagents, is amenable to scale-up, and can easily be modified to generate a wide range of n-3 and n-6 physiologically relevant VLC-PUFAs. Since synthetic VLC-PUFAs may eventually be used therapeutically in humans, we avoided the use of toxic reagents. The key features of our synthesis of 32:6 n-3 are outlined in Fig. 1*A*, and further details are provided in *SI Appendix*. Briefly, commercially available DHA (22:6 n-3) was reduced to its corresponding aldehyde and then coupled with the Grignard reagent from tetrahydropyran-protected 10-bromo-1-decanol. After dehydroxylation, deprotection, and oxidation, we were able to synthesize 32:6 n-3 on a several hundred milligram scale in 15% overall yield. This VLC-PUFA was further characterized by nuclear magnetic resonance, infrared, and mass spectrometry (MS). Gas chromatography–MS (GC-MS) analysis indicated that it was greater than 98% pure and that it coeluted with the 32:6 n-3 peak in a cow retina VLC-PUFA standard (Fig. 1*B*). A mass spectrum of the final product confirming the presence of the expected parent ion peak at 491.3857 mass/charge ratio (*m/z*) is shown in Fig. 1*C*.

We studied the bioavailability of 32:6 n-3 in wild-type (WT) mice after acute and chronic gavage feeding. Initially, mice received a single dose of 6 mg of 32:6 n-3 and were killed 0, 2, 4, 8, and 24 h later ($n = 4$ mice/time interval) to understand absorption kinetics. As shown in Fig. 2*A*, serum 32:6 n-3 became detectable within 2 h after oral administration and then reached a lower steady-state concentration over the next 24 h. A significant increase in 32:6 n-3 in the retina and RPE was observed 4 to 8 h after gavage (Fig. 2*B*). On the other hand, 32:6 n-3 remained undetectable in liver, brain, and red blood cell (RBC) membranes throughout the 24 h period.

For longer-term absorption studies, we gavage fed the WT mice for 15 d with 0, 1, and 2 mg/d 32:6 n-3 ($n = 6$ mice/group). The 32:6 n-3 levels significantly increased by more than twofold in the retina and sevenfold in RPE in both 32:6 n-3–fed groups in comparison to 0 mg/d controls (Fig. 3*A*). We also observed a significant increase ($P < 0.05$) in total retinal VLC-PUFAs in the 2 mg/d group (0.872 ± 0.10%) in comparison to the 1 mg/d (0.535 ± 0.06%) and 0 mg/d (0.531 ± 0.16%) groups. Serum and RBC VLC-PUFAs remained undetectable in the control mice and significantly increased in the 32:6 n-3–fed groups, as shown in Fig. 3*B*. The liver had detectable levels of 32:6 n-3 only in the 2 mg/d group (Fig. 3*B*), while no VLC-PUFAs were ever detectable in the brain. Further, to know whether VLC-PUFAs delivered to the eye are incorporated into phospholipid species such as phosphatidylcholine (PC) and phosphatidylethanolamine, we extracted the retina and RPE for phospholipid analysis using liquid chromatography–tandem MS (LC-MS/MS), and we detected increases in PC-22:6/32:6 in the retina and RPE in the supplemented animals (*SI Appendix*, Fig. S1). We also noted evidence of VLC-PUFA elongation, presumably by endogenous Elovl4, because by LC-MS/MS, PC-22:6/34:6 and PC-22:6/36:6 levels increased significantly in RPE and the retina, respectively (*SI Appendix*, Fig. S1).

We did not observe any systemic toxicities (hair loss, weight loss, or discoloration of organs, teeth, or nails) or abnormal social behavior in treatment groups when compared to the control groups. To confirm the absence of toxicity in the eyes, we performed electroretinography (ERG) studies comparing the 2 mg/d chronic feeding group with the 0 mg/d control group. We observed small but consistent increases in scotopic and photopic a- and b-wave amplitudes in the VLC-PUFA-fed animals, with significant improvements in scotopic ($P < 0.05$ at 20 dB) and photopic ($P = 0.01$ at 10 dB) b-wave amplitudes, suggesting that VLC-PUFA supplementation may actually improve retinal function in normal mice (Fig. 4). Functional visual improvements were confirmed by optokinetic response (OKR) experiments using OptoMotry in which scotopic and photopic visual acuities (Fig. 5) of the 2 mg/d 32:6 n-3 mice were significantly better than the control (0 mg/d) mice. Our OKR improvements in visual function in response to VLC-PUFA supplementation are comparable in magnitude to our previously reported studies of carotenoid supplementation in *Bco2* knockout (KO) mice (22).

We next used conditional KO mice developed with an intention to ablate *Elovl4* expression completely in both rods and cones (E4cKO mice). At 8 mo of age, their Elovl4 protein levels were undetectable by Western blotting (*SI Appendix*, Fig. S2). They exhibited no apparent structural degeneration by optical coherence tomography (OCT) or color fundus imaging (*SI Appendix*, Fig. S3), and histologically, they showed mild outer nuclear layer thinning relative to age-matched WT mice (*SI Appendix*, Fig. S4). Their retinal and RPE 32:6 n-3 levels were one-third and one-half of the levels in the age-matched WT mice, respectively (Fig. 6*A*). After 15 d of gavage feeding with 2 mg/d of synthetic 32:6 n-3, the 8-mo-old E4cKO mice had a nearly fivefold increase in their 32:6 n-3 levels in the retina ($P < 0.01$) and a 27-fold increase in the RPE ($P = 0.001$) relative to control-fed E4cKO mice (Fig. 6*A*). There was a significant increase ($P < 0.05$) in total retinal VLC-PUFAs in the E4cKO mice fed 2 mg/d 32:6 n-3 (0.088 ± 0.02%) in comparison to the 0 mg/d E4cKO mice (0.030 ± 0.01%) that approached the levels in age-matched 0 mg/d WT mice (0.102 ± 0.008%). Liver and RBC 32:6 n-3 became detectable in the mice fed 2 mg/d 32:6 n-3 relative to the undetectable levels in the 0 mg/d E4cKO and WT mice (Fig. 6*B*).

We then performed ERG and OKR experiments in the E4cKO mice in response to 2 mg/d 32:6 n-3 supplementation. Scotopic a- and b-waves of 8-mo-old control-fed E4cKO mice were about half the magnitude of the age-matched WT mice, and the photopic ERGs were essentially unrecordable (Fig. 7). There were improvements in scotopic and photopic a- and b-wave measurements in the 32:6 n-3–fed E4cKO group relative to the control-fed group, especially at high light intensities. When we performed OKR studies on these E4cKO mice, we observed significant improvements only in scotopic function in response to 32:6 n-3 supplementation (Fig. 8).

Discussion

VLC-PUFAs longer than 26 carbons are not present in normal vertebrate diets, yet they are uniquely found in the retina and testes, implying physiological importance of their biosynthesis from shorter-chain dietary precursors via the action of ELOVL4. While progress has been made by studying retinal samples from human donors and by investigating mouse models of Elovl4 dysfunction, further physiology and interventional research has been hampered by the scarcity of pure VLC-PUFAs. Here, we report the chemical synthesis of a VLC-PUFA (32:6 n-3) in sufficient quantity to study its bioavailability in mice and to investigate its potential roles in normal retinal function and for treatment of disorders associated with VLC-PUFA deficiency.

An earlier synthetic approach had problematic coupling reactions and use of toxic metals (21). Our reported approach (Fig. 1 and *SI Appendix*) was developed with the intention that synthetic VLC-PUFAs may someday be used therapeutically in humans, so we avoided toxic reagents. Our synthesis also has the

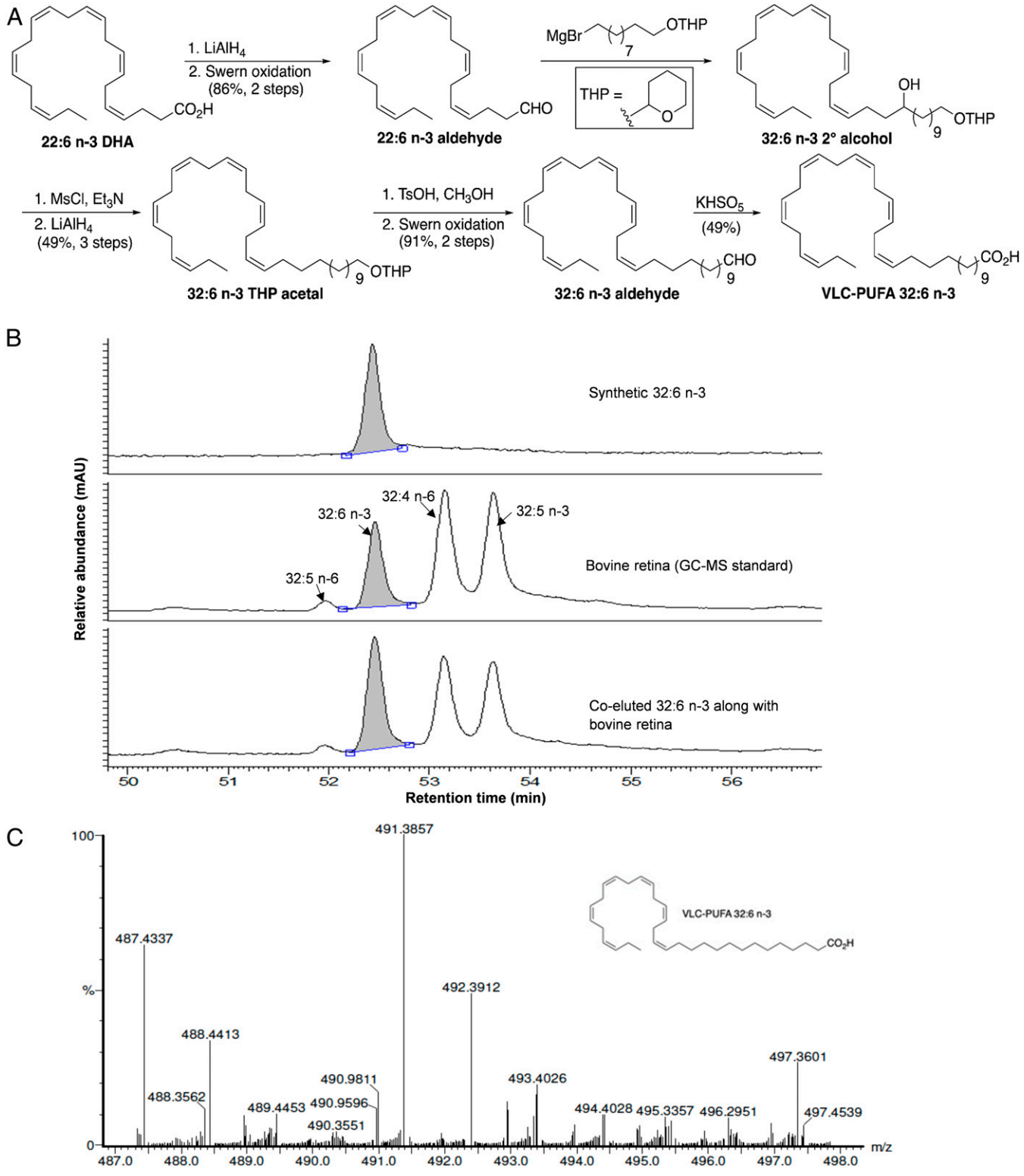

Fig. 1. Synthesis of VLC-PUFA 32:6 n-3. (*A*) Synthetic approach to 32:6 n-3. (*B*) GC-MS chromatogram of synthetic 32:6 n-3 in comparison with bovine retinal lipids. (*C*) High-resolution mass spectral confirmation of the molecular weight of the synthetic 32:6 n-3. Calculated molecular weight for $C_{32}H_{52}O_2Na$ $[M+Na]^+$ (*m/z*) 491.3865; found 491.3857.

advantage of being amenable to scale-up and can be readily modified to synthesize other n-3 and n-6 VLC-PUFA family members and isotopically labeled versions. In this study, we chose to focus on an intermediate-length 32-carbon n-3 VLC-PUFA that is present in both human and mouse retinas, but longer and shorter n-3 and n-6 versions should be examined in the future.

In view of the physiological benefits of VLC-PUFAs and the dysfunction associated with low retinal levels of VLC-PUFAs, we

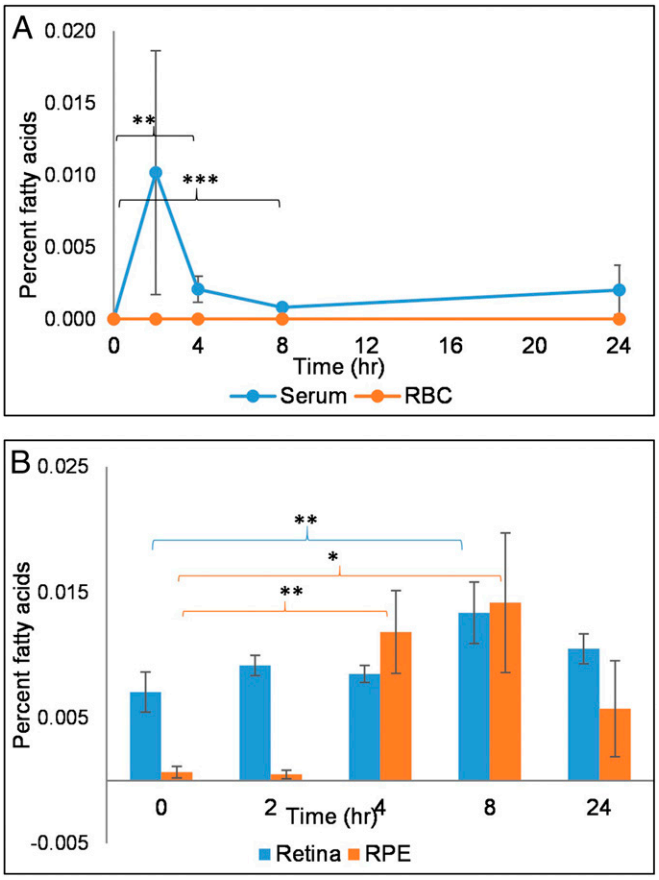

Fig. 2. WT mice single-dose bioavailability studies. (*A*) Serum absorption kinetics of 32:6 n-3 after single-dose gavage feeding of 6 mg/mouse ($n = 4$ mice/time point). (*B*) Retina and RPE uptake of 32:6 n-3 after single-dose gavage feeding. No VLC-PUFAs were detected in liver, brain, or RBC membranes at any time point. Data are presented as mean ± SEM (***$P < 0.005$; **$P < 0.01$; *$P < 0.05$).

tested the feasibility of oral delivery of a synthetic VLC-PUFA (32:6 n-3) to mouse retinas. We posited that VLC-PUFAs would be comparable to DHA in terms of bioavailability and absorption. We chose 6 mg/d of 32:6 n-3 for our single-dose study based upon earlier reports where different investigators used 2.5 to 22 mg of n-3 PUFAs per day for gavage feeding and absorption in mice (23–26). As shown in Fig. 2, serum 32:6 n-3 rapidly rose from normally undetectable levels and peaked at 2 h, and 32:6 n-3 levels rose significantly in the RPE by 4 h, while retinal increases lagged by a few hours, suggesting that exogenous VLC-PUFAs are delivered to the retina via the RPE. Other tissues such as liver, brain, and RBC membranes do not normally have detectable VLC-PUFAs and showed no short-term response to exogenous 32:6 n-3. This suggests that orally administered VLC-PUFAs may not utilize the canonical pathway of lipid uptake, which features liver-mediated incorporation into the phospholipids and triglycerides of lipoprotein particles that circulate and are taken up by the tissues.

After 15 d of gavage feeding, there were significant increases in retinal and RPE 32:6 n-3 by GC-MS (Fig. 3), and confirmatory LC-MS studies of RPE and retinal phosphatidylcholines suggested that some of the administered 32:6 n-3 is elongated (*SI Appendix*, Fig. S1), presumably by endogenous Elovl4 in these WT mice. The robust increases in RPE VLC-PUFA levels are interesting because they could serve as precursors for the neuroprotective elovanoids described by Bazan's group (27), but our analytical methods were not designed to detect the presence of these metabolites in eye tissues, so further study is warranted. RBC membranes are long-term biomarkers of dietary PUFA status (14, 28), and we confirmed a positive dose response to varying levels of long-term supplementation. In the liver, chronic feeding of our synthetic VLC-PUFA led to detectable 32:6 n-3 only in the 2 mg/d group, indicating either that liver is not a preferred site of accumulation or that it ordinarily degrades VLC-PUFAs. At higher feeding levels, the liver becomes a site for VLC-PUFA deposition, possibly because its degradation capacity is exceeded in a manner reminiscent of Zellweger syndrome, in which a peroxisomal deficiency compromises β-oxidation activity and leads to VLC–fatty acid accumulation in various tissues (29, 30). It is unclear whether these low levels of VLC-PUFAs seen in the liver in our experiments could have toxic effects, but it points out that liver function tests should be monitored in any future clinical trials with VLC-PUFAs in humans.

We used ERG and OKR to rule out retinal toxicity of exogenous VLC-PUFAs and found not only were there no toxic effects, but there were actually small, but significant, increases in ERG amplitudes and visual acuity measured by OKR (Figs. 4 and 5). Similar "supernormal" ERGs and OKRs have been reported in *Fat-1* mice fed VLC-PUFA precursors (31) and *Bco2* KO mice fed carotenoids (22). The mechanisms underlying the improvements in visual function in WT mice (i.e., changes in membrane fluidity, enhanced synaptic transmission, alterations in elovanoid levels, etc.) remain to be explored, but our findings

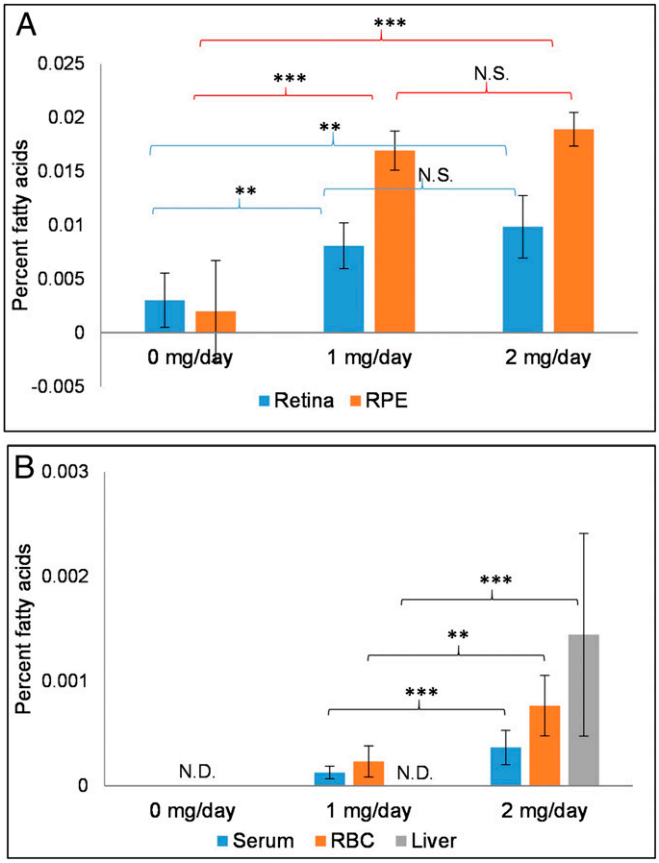

Fig. 3. WT mice repeated-dose bioavailability studies. (*A*) Accumulation of 32:6 n-3 in mouse retina and RPE after 15 d of gavage feeding ($n = 6$ mice/group). (*B*) Bioaccumulation of 32:6 n-3 in serum, RBC, and liver after 15 d of gavage feeding. No VLC-PUFAs were ever detectable in the brain. Data are presented as mean ± SEM (***$P < 0.005$; **$P < 0.01$; N.S.: not significant; N.D.: not detectable).

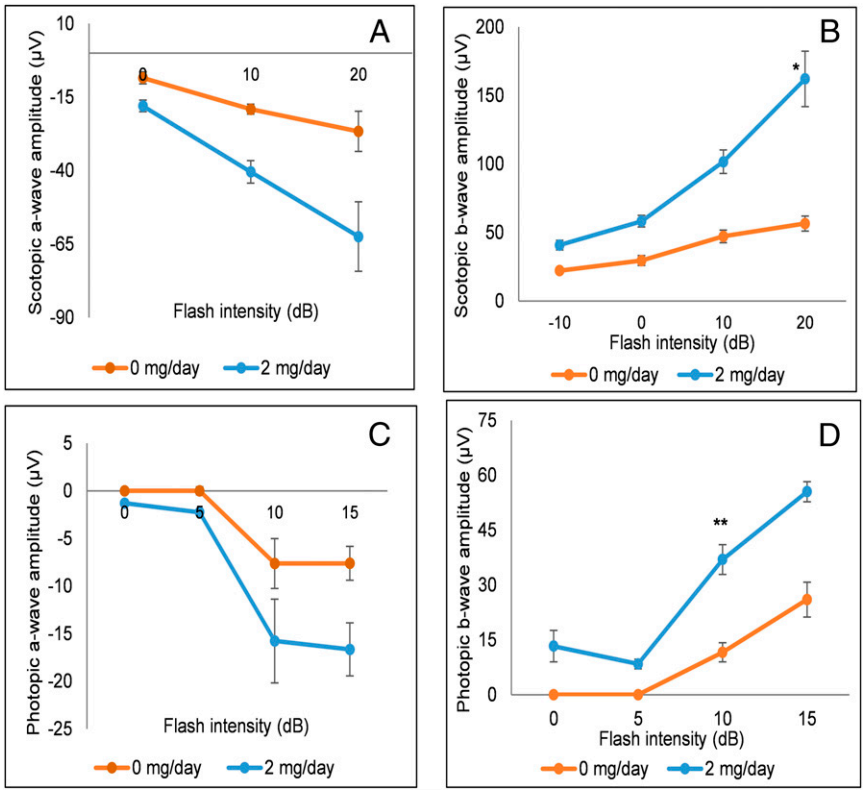

Fig. 4. WT mice ERG responses after chronic feeding with 32:6 n-3. WT mice were gavage fed with 2 mg/d of VLC-PUFA (32:6 n-3) in comparison to control animals (0 mg/d) (n = 8 mice/group). (*A*) Scotopic a-wave amplitudes. (*B*) Scotopic b-wave amplitudes. (*C*) Photopic a-wave amplitudes. (*D*) Photopic b-wave amplitudes. Data are presented as mean ± SEM (*P < 0.05; **P < 0.01).

lend strong support for the importance of VLC-PUFAs for maintenance of normal physiology of the retina.

We next examined whether or not an orally administered VLC-PUFA could ameliorate retinal dysfunction in a mouse model of VLC-PUFA deficiency. Total knockout of *Elovl4* is neonatal lethal in mice (7), and mouse models of autosomal dominant human mutations are complicated by protein mislocalization effects, so conditional knockouts are generally preferred. Published conditional knockouts, however, can take a long time to show depletion of retinal VLC-PUFAs, and there can be a disconnect between the time course of VLC-PUFA depletion and retinal dysfunction, possibly due to the relatively high levels of retinal VLC-PUFAs in laboratory mice (32, 33). Moreover, it appears important to knock out *Elovl4* in both rods and cones, probably because VLC-PUFAs can be readily transferred between cells in the retina. We chose a conditional knockout driven by promotors of rod and cone opsins (E4cKO) that turns off *Elovl4* early in life under the control rod and cone opsin promoters. As discussed in Barabas et al. (32), *Elovl4* cone cKO mice have reduced retinal VLC-PUFA content and exhibit functional deficits at about 10 mo of age. Crossbreeding these mice with *Elovl4* rod cKO mice (34) is expected to further decrease VLC-PUFA content and ERG amplitude in a manner comparable to a different *Elovl4* rod–cone cKO mouse model (34). By 8 mo of age, E4cKO mice have no detectable Elovl4 on Western blot, but they do have significantly reduced levels of VLC-PUFAs relative to age-matched WT mice and definite ERG abnormalities. We screened our 8-mo-old E4cKO mice for retinal degeneration by OCT and color fundus imaging and did not observe any retinal anomalies (*SI Appendix*, Fig. S3).

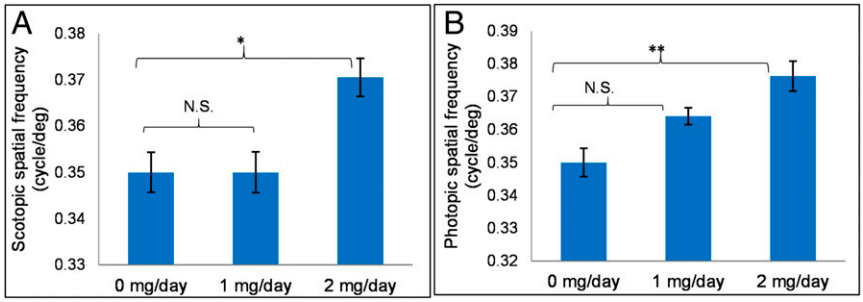

Fig. 5. WT mice OKR studies. (*A*) Improvement of scotopic spatial frequency in 32:6 n-3 gavage-fed groups (1 and 2 mg/d) in comparison to control mice (0 mg/d). (*B*) Improvement of photopic spatial frequency in gavage-fed groups in comparison to control group (n = 6 mice/group). Data are presented as mean ± SEM (**P < 0.01; *P < 0.05; N.S.: not significant).

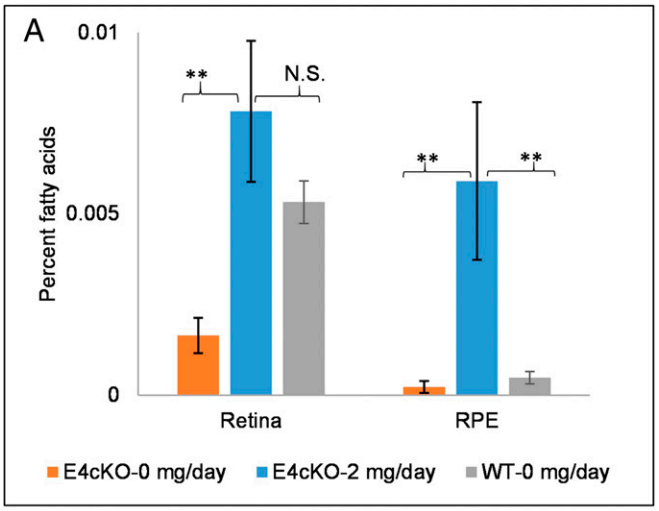

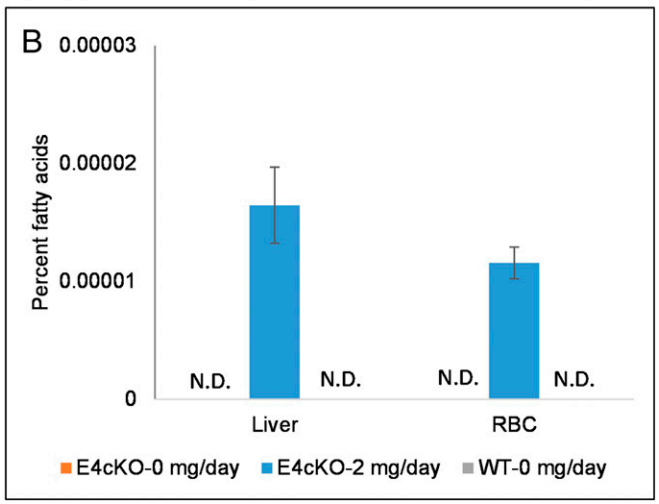

Fig. 6. Long-term uptake of 32:6 n-3 (2 mg/d per mouse) in *Elovl4* rod–cone conditional KO (E4cKO) mice. (*A*) Accumulation of 32:6 n-3 in E4cKO mouse retinas and RPE in comparison to age-matched WT mice after 15 d of gavage feeding ($n = 6$ mice/group). (*B*) Accumulation of 32:6 n-3 in liver and RBCs in E4cKO mice in comparison to age-matched WT mice after 15 d of gavage feeding. Data are presented as mean ± SEM (**$P < 0.01$; N.S.: not significant; N.D.: not detectable).

Histological studies of our E4cKO mice at 8 mo of age in comparison to WT mice displayed a slight decrease in the outer nuclear layer/total retinal thickness ratio (*SI Appendix*, Fig. S4), suggestive of a mild photoreceptor degeneration. Our findings are consistent with previous reports of other *Elovl4* knock-in and rod and/or cone conditional knockout mice that also showed ERG abnormalities and mild structural degeneration of the retina (32, 34, 35).

When we fed the E4cKO mice 2 mg/d of 32:6 n-3, we could significantly increase retinal and RPE 32:6 n-3 to levels beyond those of unsupplemented age-matched WT mice and approaching those of supplemented 3-mo-old WT mice (Fig. 6), and we could achieve partial reversal of their ERG abnormalities (Fig. 7). Visual acuity in unsupplemented E4cKO mice was not significantly impaired relative to WT mice, but like in WT mice, it improved significantly under scotopic conditions in response to VLC-PUFA supplementation, although there was no significant change photopically (Fig. 8).

While we have advanced the study of VLC-PUFAs by synthesizing one of them in sufficient quantities for small-animal research, there is still much more to be done. We have synthesized just 32:6 n-3 in quantity so far, but our synthetic scheme can be readily modified to produce n-6 and saturated analogs and shorter and longer versions with and without isotopic labels, and there is the possibility that these other compounds will have distinct physiological and pharmacological effects. Our bioavailability studies raise many interesting questions regarding how orally administered nondietary VLC-PUFAs are carried in the bloodstream and how they are selectively targeted to the retina and RPE. Our observed retinal bioavailability and improvements in retinal function in both WT and *Elovl4* conditional knockout mice are very promising, but the VLC-PUFA formulation, dosage, and timing of the intervention first need to be optimized, and then the underlying mechanisms will need to be defined. Since retinal VLC-PUFA abnormalities are also a feature of common blinding disorders such as AMD and diabetes, the potential benefits of exogenous VLC-PUFAs should be explored further.

Materials and Methods

Chemicals. All standards such as tridecanoic acid (13:0) and hentriacontanoic acid (30:0); all fatty acids methyl esters (FAMEs) such as methyl eicosanoate, methyl linolenate, methyl melissate, and Supelco-37 (a commercial mixture of FAMEs); liposome kits; α-tocopherol; and other chemicals not listed here were purchased from Sigma-Aldrich and Fisher Scientific. Silica gel, glass-encased, solid-phase extraction cartridges (500 mg/6 mL) were purchased from Sorbent Technology. DHA used for chemical synthesis was purchased from Carbosynth.

Animals. WT C57BL/6J mice were from Jackson Laboratories. *Elovl4* rod–cone conditional knockout (E4cKO) mice were developed in collaboration with David Krizaj's laboratory at the Moran Eye Center (32). To generate the conditional knockout mice with *Elovl4* deleted from both rod and cone photoreceptors, floxed-*Elovl4* mice (*Elovl4* $^{flox/flox}$) were bred with rod-specific opsin–cre (opsin–iCre75) and cone-specific human red-green pigment–cre mice, all on a C57/BL/6J background. The mice were genotyped as described in our previous report (32), and the following primers were used: Elovl4-flox, 5′-GGCGGTGGCTCATATCTTTA-3′ and 5′-CAGAAATCTGCCTGCCTCTC-3′; rod Cre, 5′-TCA GTG CCTGGA GTT GCG CTG TGG-3′ and 5′-CTT AAA GGC CAG GGC CTG CTT GGC; and cone Cre, 5′-AGG TGT AGA GAA GGC ACT TAG C-3′ and 5′- CTA ATC GCC ATC TTC CAG CAG G-3′.

Mice were housed in the vivarium at the Moran Eye Center and maintained in a standard 12 h light and 12 h dark cycle environment, with water and food ad libitum (Teklad Global Soy-Free Rodent Diet, Envigo). All animal handling procedures used in this study were approved by appropriate institutional animal care and use committees and were carried out according to NIH guidelines.

Single-Dose Gavage Experiments. VLC-PUFA-loaded liposomes were prepared using a liposome kit (0.05%) (L4395-lipid mixtures for preparation of liposomes from Sigma-Aldrich consisting of egg yolk phosphatidylcholine, stearylamine, and cholesterol in a 7:2:1 ratio) with addition of α-tocopherol (0.025%) to prevent oxidation. Three-month-old WT mice (22 ± 3 g) were gavage fed with 32:6 n-3–loaded VLC-PUFA liposomes (0.1 mL). We used a dose of 6 mg/d per mouse of 32:6 n-3 (250 mg/kg body weight [BW]), less than half the dosage used for DHA in previous studies (24–26). The mice were killed at time intervals of 0, 2, 4, 8, and 24 h after gavage ($n = 4$ mice/time point) to harvest the blood and other tissues. Eyes were dissected under a microscope to separate the retina from the RPE. One pair of retinas/mouse was used for lipid extraction, and blood was centrifuged for 5 min at 7,500 rpm to separate serum from RBCs. Serum, RBCs, brain, liver, retina, and RPE were used for lipid extractions and GC-MS analysis.

Repeated-Dose Gavage Experiments. VLC-PUFA-loaded liposomes (0.1 mL) were gavage fed daily to WT (22 ± 3 g) and E4cKO (23 ± 3 g) mice for 15 d ($n = 6$ mice/feeding group). Mice were fed each morning with liposomes prepared as described above containing 0 mg/d (0 mg/kg BW), 1 mg/d (40 mg/kg BW), or 2 mg/d (80 mg/kg BW) of 32:6 n-3. Mice were killed at the end of the experiments, and retina, RPE, liver, serum, RBCs, and brain tissues were harvested, extracted for lipids, and analyzed by GC-MS.

Electroretinograms. Full-field ERGs were recorded as described in the literature (32, 36, 37). Briefly, mice were dark adapted and anesthetized with ketamine/xylazine (90/10 mg/kg BW). The animals were placed on a heating

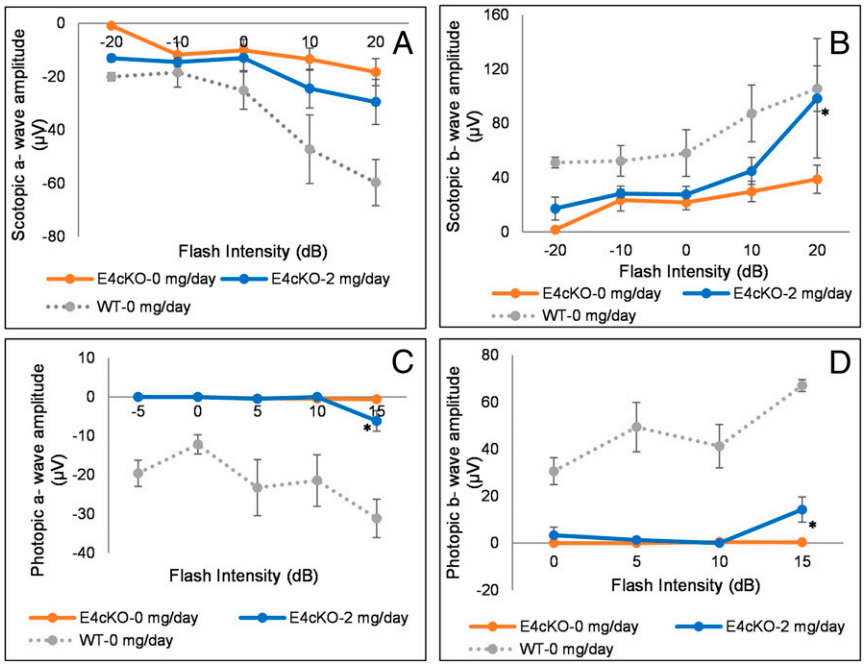

Fig. 7. ERG in 32:6 n-3–supplemented (2 mg/d per mouse) E4cKO mice. (*A*) Scotopic a-wave amplitudes. (*B*) Scotopic b-wave amplitudes. (*C*) Photopic a-wave amplitudes. (*D*) Photopic b-wave amplitudes. ERGs were recorded from E4cKO mice fed with either 2 or 0 mg/d 32:6 n-3 or age-matched WT mice fed with 0 mg/d ($n = 6$ mice/group). Data are presented as mean ± SEM (*$P < 0.05$). E4cKO 0 mg/d mice had significantly lower ERG amplitudes relative to age-matched WT mice at all spatial frequencies.

pad, and a golden ERG electrode was placed on the cornea surface. Stimuli were in order of increasing luminance from 0.00025 to 79 cd·s/m^2 (scotopic) and from 2.5 to 79 cd·s/m^2 (photopic), and 2 to 12 traces were averaged. The photoflash unit was calibrated to deliver 2.5 cd·s/m^2 at 0 dB.

Visual Behavior Testing by Optokinetic Response. Repeated-dose gavage-fed mice were tested for visual behavior to observe the effect of exogenous VLC-PUFA on vision. Since the OKR tests can be subjective, the tests were evaluated by researchers blinded to experimental treatments. Visual function and contrast sensitivity were assessed using an optokinetic testing system (OptoMotry, Cerebral Mechanics). This noninvasive method utilizes the optokinetic tracking response to assess functional vision and has been described and validated previously (38–40). The threshold of maximum spatial frequency that will result in an optokinetic tracking response is a correlate of visual acuity (39). Testing is initiated by projecting a grating of low spatial frequency (0.019 cycles/degree), rotating at 12°/s at maximum 100% contrast; that is, the bars of the gratings are maximally black, and the background is maximally white. Spatial frequency thresholds were similar when tested with one or both eyes, suggesting complete asymmetry of tracking, likely due to the absence of cortical activity during tracking motion (41).

Lipid Extraction and Purification of Lipids with Solid-Phase Extraction. Serum, RBCs, liver, brain, RPE, and retina were extracted using the procedure previously adopted in our laboratory (42). In brief, the samples were extracted in 1 mL hexane–isopropanol (3:2 vol/vol), and the extract was dried under a stream of nitrogen. The dried film was dissolved in 200 μL of hexane, and 2 mL of 4% HCl in MeOH were added and incubated at 80 °C for 4 h to form FAMEs (42). The FAME mixture was extracted three times with 1 mL distilled water and 2 mL hexane, and the hexane layers were combined and dried under nitrogen gas. Silica gel, glass-encased, solid-phase extraction cartridges were subsequently used to clean the FAME extracts. FAMEs were eluted from the cartridge with hexane–ether (4:1 vol/vol), and the eluate was evaporated under nitrogen gas. The dry film was dissolved in 200 μL of hexane, and 1 μL of sample was injected into the GC-MS instrument for LC-PUFA and VLC-PUFA analyses.

GC-MS Instrumentation and Chromatographic Conditions. We used either a Thermo Trace GC-DSQ II system (ThermoFisher Scientific) consisting of an automatic sample injector (AS 3000), gas chromatograph (GC), and a single quadrupole mass detector or an Agilent instrument (Agilent Technologies) equipped with 5977B mass spectrometer, an 8890 GC, and an autosampler. Both systems were operated with Xcaliber and Chemstation software. The chromatographic separation was carried out with an Rxi-5MS coated 5% diphenyl/95% dimethyl polysiloxane capillary column (30 m × 0.25 mm internal diameter, 0.25 μm film thickness) (Restek). Two methods (A and B) were used for detection and quantitation of LC-PUFAs and VLC-PUFAs, respectively, as previously published (42). Bovine retina VLC-PUFAs were extracted and employed as VLC-PUFA standards to establish retention times because commercial standards are not available, and identification of each VLC-PUFA in retinal samples was achieved as described in prior work from our laboratory. Peak areas were normalized with reference to internal standards, and sample weight and the mole percentage were calculated as published earlier from our laboratory (43). All the fatty acid levels in this study are expressed in mole percent of total fatty acids.

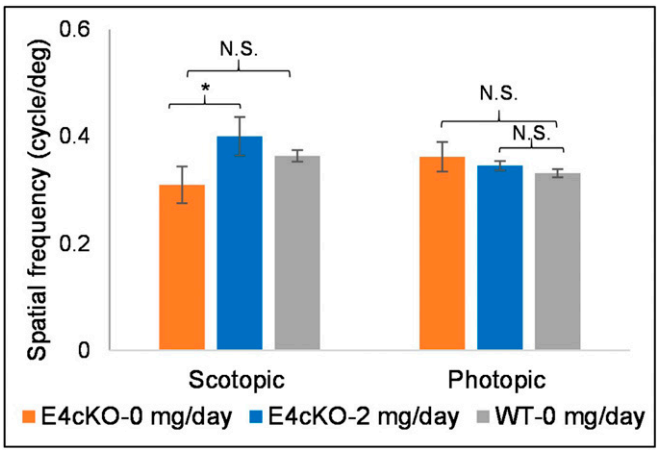

Fig. 8. OKR in 32:6 n-3–supplemented (2 mg/d per mouse) E4cKO mice. Scotopic and photopic visual acuities in 2 mg/d 32:6 n-3–fed E4cKO mice in comparison to control E4cKO mice (0 mg/d 32:6 n-3) and age-matched WT mice (0 mg/d 32:6 n-3) ($n = 6$ mice/group). Data are presented as mean ± SEM (*$P < 0.05$; N.S.: not significant).

LC-MS/MS. Lipid extractions on retinal and RPE extracts were done using Harkewicz et al.'s (34) procedure. See *SI Appendix* for detailed extraction and analysis.

Statistical Analyses. Statistical analyses were performed using ANOVA and two-sided *t* tests on Prism software (GraphPad Software). Data are represented as the mean ± SEM. Significance is indicated by *P* value measurements, with $P < 0.05$ considered significant.

Data Availability. All study data are included in the article and/or *SI Appendix*.

ACKNOWLEDGMENTS. This work was supported by a Knights Templar Career starter grant (A.G.), a University of Utah Center on Aging Seed grant (J.D.R.), Foundation Fighting Blindness Grant TA-NMT-0618-0736-UUT (P.S.B.), a Carl Marshall Reeves and Mildred Almen Reeves Foundation grant (P.S.B.), and departmental core grants from Research to Prevent Blindness and NIH (Grant EY14800). We thank Aniket Ramsekhar and Dr. Haibo Wang for their help with histology.

1. L. D. Bennett *et al*., Examination of VLC-PUFA-deficient photoreceptor terminals. *Invest. Ophthalmol. Vis. Sci.* **55**, 4063–4072 (2014).
2. M. I. Aveldaño, Phospholipid species containing long and very long polyenoic fatty acids remain with rhodopsin after hexane extraction of photoreceptor membranes. *Biochemistry* **27**, 1229–1239 (1988).
3. B. R. Hopiavuori, R. E. Anderson, M. P. Agbaga, ELOVL4: Very long-chain fatty acids serve an eclectic role in mammalian health and function. *Prog. Retin. Eye Res.* **69**, 137–158 (2019).
4. M. P. Agbaga, S. Logan, R. S. Brush, R. E. Anderson, Biosynthesis of very long-chain polyunsaturated fatty acids in hepatocytes expressing ELOVL4. *Adv. Exp. Med. Biol.* **801**, 631–636 (2014).
5. P. S. Bernstein *et al*., Diverse macular dystrophy phenotype caused by a novel complex mutation in the ELOVL4 gene. *Invest. Ophthalmol. Vis. Sci.* **42**, 3331–3336 (2001).
6. K. Zhang *et al*., A 5-bp deletion in ELOVL4 is associated with two related forms of autosomal dominant macular dystrophy. *Nat. Genet.* **27**, 89–93 (2001).
7. V. Vasireddy *et al*., Loss of functional ELOVL4 depletes very long-chain fatty acids (> or =C28) and the unique ω-O-acylceramides in skin leading to neonatal death. *Hum. Mol. Genet.* **16**, 471–482 (2007).
8. W. Li *et al*., Depletion of ceramides with very long chain fatty acids causes defective skin permeability barrier function, and neonatal lethality in ELOVL4 deficient mice. *Int. J. Biol. Sci.* **3**, 120–128 (2007).
9. F. Deák, R. E. Anderson, J. L. Fessler, D. M. Sherry, Novel cellular functions of very long chain-fatty acids: Insight from ELOVL4 mutations. *Front. Cell. Neurosci.* **13**, 428 (2019).
10. A. Gorusupudi, A. Liu, G. S. Hageman, P. S. Bernstein, Associations of human retinal very long-chain polyunsaturated fatty acids with dietary lipid biomarkers. *J. Lipid Res.* **57**, 499–508 (2016).
11. A. Gorusupudi, F. Y. Chang, K. Nelson, G. S. Hageman, P. S. Bernstein, n-3 PUFA supplementation alters retinal very-long-chain-PUFA levels and ratios in diabetic animal models. *Mol. Nutr. Food Res.* **63**, e1801058 (2019).
12. M. Tikhonenko *et al*., Remodeling of retinal fatty acids in an animal model of diabetes: A decrease in long-chain polyunsaturated fatty acids is associated with a decrease in fatty acid elongases Elovl2 and Elovl4. *Diabetes* **59**, 219–227 (2010).
13. D. Chen *et al*., The lipid elongation enzyme ELOVL2 is a molecular regulator of aging in the retina. *Aging Cell* **19**, e13100 (2020).
14. A. F. Hubbard, E. W. Askew, N. Singh, M. Leppert, P. S. Bernstein, Association of adipose and red blood cell lipids with severity of dominant Stargardt macular dystrophy (STGD3) secondary to an ELOVL4 mutation. *Arch. Ophthalmol.* **124**, 257–263 (2006).
15. J. M. Seddon *et al*., Dietary fat and risk for advanced age-related macular degeneration. *Arch. Ophthalmol.* **119**, 1191–1199 (2001).
16. J. P. SanGiovanni *et al*.; Age-Related Eye Disease Study Research Group, The relationship of dietary omega-3 long-chain polyunsaturated fatty acid intake with incident age-related macular degeneration: AREDS report no. 23. *Arch. Ophthalmol.* **126**, 1274–1279 (2008).
17. B. Chua *et al*., Dietary fatty acids and the 5-year incidence of age-related maculopathy. *Arch. Ophthalmol.* **124**, 981–986 (2006).
18. Age-Related Eye Disease Study 2 Research Group, Lutein + zeaxanthin and omega-3 fatty acids for age-related macular degeneration: The age-related eye disease study 2 (AREDS2) randomized clinical trial. *JAMA* **309**, 2005–2015 (2013).
19. R. Choi, A. Gorusupudi, P. S. Bernstein, Long-term follow-up of autosomal dominant Stargardt macular dystrophy (STGD3) subjects enrolled in a fish oil supplement interventional trial. *Ophthalmic Genet.* **39**, 307–313 (2018).
20. M.-P. Agbaga *et al*., Role of Stargardt-3 macular dystrophy protein (ELOVL4) in the biosynthesis of very long chain fatty acids. *Proc. Natl. Acad. Sci. U.S.A.* **105**, 12843–12848 (2008).
21. G. M. Maharvi, A. O. Edwards, A. H. Fauq, Chemical synthesis of deuterium-labeled and unlabeled very long chain polyunsaturated fatty acids. *Tetrahedron Lett.* **51**, 6426–6428 (2010).
22. B. Li *et al*., Supplementation with macular carotenoids improves visual performance of transgenic mice. *Arch. Biochem. Biophys.* **649**, 22–28 (2018).
23. P. K. Yip *et al*., The omega-3 fatty acid eicosapentaenoic acid accelerates disease progression in a model of amyotrophic lateral sclerosis. *PLoS One* **8**, e61626 (2013).
24. R. D. C. C. de Sá *et al*., Fish oil prevents changes induced by a high-fat diet on metabolism and adipokine secretion in mice subcutaneous and visceral adipocytes. *J. Physiol.* **594**, 6301–6317 (2016).
25. K. Limbkar *et al*., Data on the effect of oral feeding of arachidonic acid or docosahexanoic acid on haematopoiesis in mice. *Data Brief* **14**, 551–557 (2017).
26. L. H. Jiang, Y. Shi, L. S. Wang, Z. R. Yang, The influence of orally administered docosahexaenoic acid on cognitive ability in aged mice. *J. Nutr. Biochem.* **20**, 735–741 (2009).
27. B. Jun *et al*., Elovanoids are novel cell-specific lipid mediators necessary for neuroprotective signaling for photoreceptor cell integrity. *Sci. Rep.* **7**, 5279 (2017).
28. B. M. Merle *et al*.; Nutritional AMD Treatment 2 Study Group, Circulating omega-3 fatty acids and neovascular age-related macular degeneration. *Invest. Ophthalmol. Vis. Sci.* **55**, 2010–2019 (2014).
29. A. E. Moser *et al*., The cerebrohepatorenal (Zellweger) syndrome. Increased levels and impaired degradation of very-long-chain fatty acids and their use in prenatal diagnosis. *N. Engl. J. Med.* **310**, 1141–1146 (1984).
30. A. Poulos, P. Sharp, D. Johnson, C. Easton, The occurrence of polyenoic very long chain fatty acids with greater than 32 carbon atoms in molecular species of phosphatidylcholine in normal and peroxisome-deficient (Zellweger's syndrome) brain. *Biochem. J.* **253**, 645–650 (1988).
31. M. Suh, Y. Sauvé, K. J. Merrells, J. X. Kang, D. W. L. Ma, Supranormal electroretinogram in fat-1 mice with retinas enriched in docosahexaenoic acid and n-3 very long chain fatty acids (C24-C36). *Invest. Ophthalmol. Vis. Sci.* **50**, 4394–4401 (2009).
32. P. Barabas *et al*., Role of ELOVL4 and very long-chain polyunsaturated fatty acids in mouse models of Stargardt type 3 retinal degeneration. *Proc. Natl. Acad. Sci. U.S.A.* **110**, 5181–5186 (2013).
33. L. D. Bennett *et al*., Effect of reduced retinal VLC-PUFA on rod and cone photoreceptors. *Invest. Ophthalmol. Vis. Sci.* **55**, 3150–3157 (2014).
34. R. Harkewicz *et al*., Essential role of ELOVL4 protein in very long chain fatty acid synthesis and retinal function. *J. Biol. Chem.* **287**, 11469–11480 (2012).
35. A. McMahon *et al*., Retinal pathology and skin barrier defect in mice carrying a Stargardt disease-3 mutation in elongase of very long chain fatty acids-4. *Mol. Vis.* **13**, 258–272 (2007).
36. J. L. Duncan *et al*., Scotopic visual signaling in the mouse retina is modulated by high-affinity plasma membrane calcium extrusion. *J. Neurosci.* **26**, 7201–7211 (2006).
37. O. Yarishkin, T. T. T. Phuong, M. Lakk, D. Križaj, TRPV4 does not regulate the distal retinal light response. *Adv. Exp. Med. Biol.* **1074**, 553–560 (2018).
38. G. T. Prusky, N. M. Alam, S. Beekman, R. M. Douglas, Rapid quantification of adult and developing mouse spatial vision using a virtual optomotor system. *Invest. Ophthalmol. Vis. Sci.* **45**, 4611–4616 (2004).
39. R. M. Douglas *et al*., Independent visual threshold measurements in the two eyes of freely moving rats and mice using a virtual-reality optokinetic system. *Vis. Neurosci.* **22**, 677–684 (2005).
40. G. T. Prusky, N. M. Alam, R. M. Douglas, Enhancement of vision by monocular deprivation in adult mice. *J. Neurosci.* **26**, 11554–11561 (2006).
41. S. L. Burroughs, S. Kaja, P. Koulen, Quantification of deficits in spatial visual function of mouse models for glaucoma. *Invest. Ophthalmol. Vis. Sci.* **52**, 3654–3659 (2011).
42. A. Liu, R. Terry, Y. Lin, K. Nelson, P. S. Bernstein, Comprehensive and sensitive quantification of long-chain and very long-chain polyunsaturated fatty acids in small samples of human and mouse retina. *J. Chromatogr. A* **1307**, 191–200 (2013).
43. A. Liu, J. Chang, Y. Lin, Z. Shen, P. S. Bernstein, Long-chain and very long-chain polyunsaturated fatty acids in ocular aging and age-related macular degeneration. *J. Lipid Res.* **51**, 3217–3229 (2010).